British Journal of Pharmacology (2006) 149, 676–686
 0007–1188/06 $30.00
www.brjpharmacol.org

RESEARCH PAPER

Pharmacological and molecular evidence for the involvement of $K_v4.3$ in ultra-fast activating K^+ currents in murine portal vein myocytes

SYM Yeung[1], S Ohya[2], GP Sergeant[3], V Pucovský[1] and IA Greenwood[1]

[1]*Division of Basic Medical Sciences, Ion Channels and Cell Signalling Research Centre, St George's, University of London, London, UK;* [2]*Department of Molecular and Cellular Pharmacology, Graduate School of Pharmaceutical Sciences, Nagoya City University, Japan and* [3]*Smooth Muscle Research Centre, Dundalk Institute of Technology, Dundalk, Co Louth, Ireland*

Background and purpose: The aim of this study was to determine the molecular identity of a transient K^+ current (termed I_{UF}) in mouse portal vein myocytes using pharmacological and molecular tools.
Experimental approach: Whole cell currents were recorded using the ruptured patch con from either acutely dispersed single smooth muscle cells from the murine portal vein or human embryonic kidney cells. Reverse transcriptase polymerase reaction (RT-PCR) experiments were undertaken on RNA isolated from mouse portal vein using primers specific for various voltage-dependent K^+ channels, auxillary subunits and calcium-binding proteins. Immunocytochemistry was undertaken using an antibody specific for $K_v4.3$.
Key results: I_{UF} had a mean amplitude at $+40$ mV of 558 ± 50 pA ($n = 32$) with a mean time to peak at $+40$ mV of ~ 4 ms. I_{UF} activated and inactivated with a half maximal voltage of -12 ± 2 mV and -85 ± 2 mV, respectively. I_{UF} was relatively resistant to 4-aminopyridine (5 mM produced 30 ± 6 % block at $+20$ mV) but was inhibited effectively by flecainide (IC_{50} value was 100nM) and phrixotoxin II. This pharmacological profile is consistent with I_{UF} being comprised of $K_v4.x$ proteins and this is supported by the results from the quantitative PCR and immunocytochemical experiments.
Conclusions and implications: These data represent a rigorous investigation of the molecular basis of vascular transient K^+ currents and implicates $K_v4.3$ as a major component of the channel complex.
British Journal of Pharmacology (2006) **149,** 676–686. doi:10.1038/sj.bjp.0706903; published online 3 October 2006

Keywords: K_v4, transient potassium current; vascular smooth muscle; Q-PCR; immunocytochemistry

Abbreviations: 4-AP, 4-aminopyridine; IC_{50}, concentration that produces 50% inhibition; I_{UF}, ultra-fast activating, transient K^+ current; mPV, murine portal vein; PaTx2, phrixotoxin II; V_H, holding potential; V_T, test potential

Introduction

Voltage-dependent, calcium-independent potassium (K^+) channels are present in all smooth muscle cells and are subdivided broadly on the basis of their time dependence into rapidly activating and inactivating A-type currents and slower activating delayed rectifiers. A-type currents have been studied extensively in the neurons where they were initially identified (Connor and Stevens, 1971) and where they regulate action potential discharge frequency. A-type currents are also present in smooth muscle cells although not ubiquitously (see Amberg *et al*., 2003), and their role is less clearly defined because of their relatively negative inactivation relative to the more positive resting membrane potential of smooth muscle cells (about -50 mV). Various K^+ channel gene products generate K^+ channels with properties resembling A-type currents. These include $K_v1.4$, $K_v3.4$ and $K_v4.1$–4.3 (Amberg *et al*., 2003). Extensive studies in mouse colon and antrum have implicated $K_v4.2$ and $K_v4.3$ gene products as constituents of A-type channels (Amberg *et al*., 2002a, b). These studies also showed the expression of members of the recoverin–neuronal calcium sensor super-family especially NCS-1 and various KChIPs (K^+ channel interacting protein), which are known to influence $K_v4.x$ expression, surface presentation and biophysical properties (Birnbaum *et al*., 2004).

A-type currents are also apparent in various vascular smooth muscle cells types (see Amberg *et al*., 2003). However, there is considerable equivocation as to the molecular identity of the A-type channels in the vasculature. Iida *et al*. (2005) have identified $K_v3.4$ and K_v4 gene expression products in human cultured pulmonary artery myocytes and proposed that two distinct transient currents

Correspondence: Dr IA Greenwood, Division of Basic Medical Sciences, Ion Channels And Cell Signalling Research Centre, St George's, University of London, London SW 17 0RE, UK. E-mail: i.greenwood@sgul.ac.uk
Received 16 May 2006; revised 25 July 2006; accepted 15 August 2006; published online 3 October 2006

are present in these cells. However, culturing conditions are known to alter gene expression and electrophysiological profiles. Notably, Miguel-Velado *et al*. (2005) demonstrated that phenotypically different K^+ currents can be recorded from acutely dispersed human uterine artery myocytes compared to cultured myocytes and this was associated with an upregulation in $K_v3.4$ expression. The aim of the present study was to ascertain whether $K_v4.x$ gene products constituted the transient K^+ channels in murine portal vein (mPV), a cell type previously shown to exhibit a robust A-type current (Beech and Bolton, 1989). We show through a combination of pharmacological profile and molecular techniques that $K_v4.3$ is the most likely candidate for the transient current in these cells but the native current differs in various ways from heterologously expressed $K_v4.3$ suggesting a combination with protein partners.

Methods

Mouse portal vein (mPV) smooth muscle cells were dissociated freshly from 6- to 8-week-old female BALB/c mice (Britton *et al*., 2002). Animals were killed by cervical dislocation, the portal vein removed and bathed in physiological saline solution (PSS) containing 1 mM Ca^{2+}. Isolated cells were obtained enzymatically by treating the tissue with 100 μM Ca^{2+} PSS containing 0.3 mg ml^{-1} protease (type XIV, Sigma, Poole, Dorset, UK); then with 0.6 mg ml^{-1} collagenase (type I, Calbiochem, Nottingham, UK), both at 37°C for 6 min. Dispersed cells were kept on ice until required. Whole cell currents were recorded at room temperature (20–22°C) using the conventional, ruptured-patch configuration of the whole cell technique. To study voltage-gated K^+ currents in isolation, ethylene glycol-bis-(2-aminoethyl ether)-*N*,*N*,*N*′,*N*′-tetraacetic acid (EGTA) (5 mM) and ATP (3 mM) were included in the pipette solution. This rationale has been used in a number of studies (e.g. Akbarali *et al*., 1999; Platoshyn *et al*., 2004; Yeung and Greenwood, 2005) to eliminate any contribution from Ca^{2+}-activated K^+ currents, especially of the large conductance type (BK_{Ca}) and ATP-sensitive K^+ (K_{ATP}) currents to the overall outward conductance. The ultra-fast activating current (termed I_{UF}) was identified by digitally subtracting currents recorded at test potentials (V_T) between –80 and + 40 mV from a holding potential (V_H) of –60 mV from those evoked at the same V_T but following a 1 s prepulse to –90 mV (see Beech and Bolton, 1989). All recordings were sampled at 2 kHz and low-pass filtered at 1 kHz. However, the effective low-pass filtering frequency was 700 Hz given by the RC filter of the membrane based upon a mean uncompensated cell capacitance and series resistance of 19.6 ± 0.9 pF and 11.6 ± 0.6 MΩ ($n = 23$). Data were acquired by use of an Axopatch 200B amplifier, Digadata 1322A interface and pClamp (version 9, Axon Instruments, Foster City, CA, USA). Data were analysed using Clampfit (Axon Instruments), Origin (version 6, Microcal, USA) and Excel (Microsoft, USA). All data were obtained from >2 animals.

Table 1 Oligonucleotide sequence of primers used for Q-PCR on K^+ channel α-subunits

Gene	*Primer sequence (+): sense, (−): antisense*	*Primer site*	*Product length (bp)*
Kv1.1	(+) 5′-AGCTCAAGACTCTGGCACAGTTC-3′	1224–1246	147
	(−) 5′-CCCCGGACTGGTAGTAATAAAGG-3′	1348–1370	
Kv1.2	(+) 5′-GACAGGTGTGGCTTCTCTTTGAAT-3′	1123–1146	101
	(−) 5′-GAAGCTGACGATGGAGATCAGA-3′	1202–1223	
Kv1.3	(+) 5′-AGGTGTCTTGACCATTGCATTG-3′	1260–1281	101
	(−) 5′-GCATGTACTGGGCTTGCTCTT-3′	1340–1360	
Kv1.4	(+) 5′-GTGTCTGTCCTGGTCATCTTAATCTC-3′	2135–2160	101
	(−) 5′-CCTGCACTGAGGGCCATAATA-3′	2215–2235	
Kv1.5	(+) 5′-GGATGAAGGCTTCATCAAGGAA-3′	867–888	129
	(−) 5′-AAGACCGACACGATGGCAAT-3′	976–995	
Kv1.6	(+) 5′-GACAGGTCTGGCTTCTCTTTGAGTAC-3′	743–768	104
	(−) 5′-AATTGAGGCAAGGTCTCCAGGC-3′	825–846	
Kv1.7	(+) 5′-AGGCATTCGAAGGGTCTACAGA-3′	1366–1387	123
	(−) 5′-AAGTAGACTGCGCTGGAAAAGAG-3′	1462–1484	
Kv2.1	(+) 5′-TCTCCAGCCTGGTCTTCTTTG-3′	1210–1310	144
	(−) 5′-CGATTTTCCCCAGGAGAGTCT-3′	1333–1353	
Kv3.1	(+) 5′-CCCCAACAAGGTGGAATTCA-3′	937–956	102
	(−) 5′-TTTGAGGACAGGCCGCTTA-3′	1020–1038	
Kv3.2	(+) 5′-TGGCAAGCTCGCCTACATTT -3′	851–870	101
	(−) 5′-ATGTTCCAGAAGCCGGTTTTC-3′	931–951	
Kv3.3	(+) 5′-CAGACAGAAAGGACAAGTGGCTAGA-3′	1863–1887	100
	(−) 5′-TGGCTGAAATCCGTGTTCAC-3′	1943–1962	
Kv3.4	(+) 5′-GGTGGGATTGAGTGGTTTGTCT-3′	1004–1025	108
	(−) 5′-AAGTGGCGTGTGAGCTTGAA-3′	1092–1111	
Kv4.1	(+) 5′-GCCGCTCTGCTTTTGAACA-3′	1409–1427	101
	(−) 5′-AAGGGCCTCACTGAAAGTTAGCT-3′	1487–1509	
Kv4.2	(+) 5′-CCAAAAACCATAGCAGGGAAGA-3′	1322–1343	101
	(−) 5′-CGACTGAAGTTCGACACGATCA-3′	1401–1422	
Kv4.3	(+) 5′-AGTTCACAAGCATCCCTGCAT-3′	1049–1069	103
	(−) 5′-CCAAATATCTTCCCTGCGATTG-3′	1130–1151	
GAPDH	(+) 5′-CATGGCCTTCCGTGTTCCT-3′	730–749	104
	(−) 5′-CCTGCTTCACCACCTTCTTGA-3′	814–833	

Abbreviations: GAPDH, glyceraldehyde-3-phosphate dehydrogenase; Q-PCR, quantitative, real-time polymerase chain reaction.

Quantitative polymerase chain reaction

RNA was isolated as previously reported (Ohya *et al*., 2002) using the SNAP RNA isolation kit (Invitrogen, San Diego, CA, USA). Real-time quantitative polymerase chain reaction (PCR) was performed using Syber Green chemistry with an ABI 7000 sequence detector (Applied Biosystems, Foster City, CA, USA). Unknown quantities relative to the standard curve for a particular set of primers were calculated, yielding transcriptional quantification of gene products relative to the endogenous standard (glyceraldehyde-3-phosphate dehydrogenase (GAPDH)). The reproducibility of the assay was tested by analysis of variance (ANOVA) comparing repeat runs of samples from four different animals, and mean values generated at individual time points were compared by Student's *t*-test. Table 1 shows the PCR primers used for real-time PCR analysis. PCR primers were designed using Primer Express Ver. 2.0 (Applied Biosystems) or Genetyx-Win software (Genetyx, Tokyo Japan), sequence homology analysed by NCBI-BLAST (NIH, USA) and are listed in Tables 1 and 2. Amplified products were sequenced using BigDye terminator v3 kit (Applied Biosystems) with an ABI PRIZM 3100 genetic analyzer (Applied Biosystems).

Immunocytochemistry. The cells were prepared as described previously (Saleh *et al*., 2005) and imaged using a laser scanning confocal microscope. The cells were labelled with antibodies specific for $K_v4.3$ (Santa Cruz Biotechnology Inc., USA) in dilution of either 1:100 or 1:200 and the labelling was visualized with Alexa Fluor 633-conjugated donkey anti-goat antibodies (1:500, Invitrogen). The specificity of this antibody was confirmed by Western blot analysis of protein extract form murine heart (manufacturers data sheet, sc-11686) and also by Doronin *et al.* (2004) using heart extract and human embryonic kidney (HEK) cells over expressing $K_v4.3$. In control experiments the primary antibodies were preincubated for at least 15 min with antigenic peptide (in a 1:2 ratio; length of approximately 20 amino-acid residues, mapping an intracellular epitope between amino-acid residues 550 and 600 of $K_v4.3$). PSS contained penicillin ($20\,U\,ml^{-1}$) and streptomycin ($20\,\mu g\,ml^{-1}$) at all times during immunocytochemical experiments. The cells were imaged using a Zeiss LSM 510 laser scanning confocal microscope (Carl Zeiss, Jena, Germany). The excitation beam was produced by a helium–neon laser (633 nm) and delivered to the specimen via a Zeiss Apochromat $\times 63$ oil immersion objective (numerical aperture 1.4). Emitted fluorescence was captured using LSM 510 software (release 3.2, Carl Zeiss, Jena, Germany). The cells were scanned in three dimensions as a z-stack of two-dimensional images (512×512 pixels) $0.1\,\mu m$ apart.

Table 2 Oligonucleotide sequence of primers used for Q-PCR on K^+ channel accessory proteins and calcium binding proteins

Gene	*Primer sequence (+): sense, (−): antisense*	*Primer site*
Kvβ1	(+) 5′-GATGGAGATCATGGAAGCCTACTC-3′	1066–1089
	(−) 5′-CCACCTTCTCTCTCTGGAAAAGAT-3′	1143–1166
Kvβ2	(+) 5′-TGAGATGGCAGAGCACCTAATG-3′	333–354
	(−) 5′-ACCGTCTCCATCCCTTCTTCTTA-3′	444–466
Kvβ3	(+) 5′-GGCAGGAAAGGCTGAAAGAA-3′	821–840
	(−) 5′-GCCTGTCCACCCCAAAAAAT-3′	903–922
NCS1	(+) 5′-AGCTGGATGCCGCTGGTTTC-3′	128–147
	(−) 5′-GGGTCCCCCTTGAGGTCACC-3′	273–292
GCAP1	(+) 5′-CCATGGGCAACGTCATGGAG-3′	21–40
	(−) 5′-TGGCTGAGGGGCTCAGGTTC-3′	160–179
GCAP2	(+) 5′-CTGGAGTATGTGGCAGCCCTGAA-3′	322–344
	(−) 5′-CGCCTCCACAATGTCCAGGA-3′	437–456
Hippocalcin	(+) 5′-AGCAAGCTGCGGCCAGAGAT-3′	16–35
	(−) 5′-AAACTTGGAGGCGTCGCCAT-3′	173–192
NVP1	(+) 5′-TCAAGGACTGTCCGAGCGGG-3′	104–123
	(−) 5′-TGGAGGTGATGGACAGGGCA-3′	261–280
NVP2	(+) 5′-ACACGGAGTTCAGCGAGCAGG-3′	217–237
	(−) 5′-GGTGCCATCGCCGTTCTTGT-3′	379–398
NVP3	(+) 5′-CAAGCTGCGTCCTGAGGTGC-3′	251–270
	(−) 5′-AGGCATCGCCGTAGGGGAAG-3′	398–417
Recoverin	(+) 5′-AGCAAGAGCGGTGCCCTGTC-3′	109–128
	(−) 5′-ACTTTCGAACTCCTGCCGCG-3′	233–252
KChIP1	(+) 5′-ACCGGCCTGAGGGACTGGAG-3′	437–456
	(−) 5′-GCTGGCATCTCCGTGAGGGA-3′	581–600
KChIP2	(+) 5′-TCCCAGCGGAATCGTCAATG -3′	354–373
	(−) 5′-TCACCGACAAGCCAGCCACA-3′	495–514
KChIP3	(+) 5′-GGGCGCATACCACTGAGCAA-3′	176–195
	(−) 5′-CTGATGGCGCACCGTGGATA-3′	320–339
KChIP4	(+) 5′-GAGGCCCAGAGCAAATTCACCA-3′	229–250
	(−) 5′-TCCATTGTGGTCCGTGTCGAA-3′	395–414

Abbreviation: Q-PCR, quantitative, real-time polymerase chain reaction.

Analysis of data. The procedure used for image analysis was as described previously (Saleh *et al*., 2005). Briefly, an image cutting horizontally through approximately the middle of the cell was selected out of a z-stack of images. To assess the cellular distribution of $K_v4.3$ channels a circular area of $1\,\mu m^2$ (diameter approx. $1.1\,\mu m$) was randomly selected in the subplasmalemmal area of the cell (referred to as Region 1 in Figure 5a). Another circular area of $1\,\mu m^2$ (Region 2) was selected so that the perimeter of that circle touched the perimeter of Region 1 and the line going through the centres of these circles was perpendicular to the edge of the cell, thought to be the plasma membrane. The percentage of fluorescing pixels (%FP) was calculated in both Regions using the formula

$$\%FP = 100 \times \frac{n(p > \text{threshold})}{n(p)}$$

where $n(p > \text{threshold})$ is the number of pixels within the Region whose intensity equalled or exceeded the threshold value (one standard deviation of the pixel intensities in the image) and $n(p)$ the total number of pixels in the Region. The pixels with intensities from 0 to lower than the value of one standard deviation were considered to have zero value in order to minimize the background (mainly photomultiplier) noise. The %FP values were then compared with each other and with the %FP in the whole confocal plane of the cell. The average pixel fluorescence (APF) value was used to compare the overall fluorescence signal between the staining and its controls and was calculated using the formula:

$$APF = \frac{\sum i(p)}{n(p)} (IU/\text{pixel})$$

where $i(p)$ is the intensity of a pixel within the confocal plane of the cell and $n(p)$ is the total number of pixels of the plane. Statistical evaluation and graphs were performed

using MicroCal Origin software (MicroCal Software Inc., USA) and final images were produced using CorelDraw 10 software (Corel Corporation, Canada).

Expression of $K_v4.3$ in HEK-293 cells. The full length of rat $K_v4.3$ was ligated into the mammalian expression vector pcDNA3.1 using T4 DNA ligase (New England BioLabs, Beverly, MA, USA). Successful cloning into this vector was confirmed by DNA sequencing. HEK-293 cells were transfected with the vector using the calcium phosphate method and cell lines that stably expressed $K_v4.3$ were obtained by G418 selection (Invitrogen, San Diego, CA, USA).

Solutions and reagents

PSS contained (mM): NaCl (125), KCl (5.4), $NaHCO_3$ (15.4), Na_2HPO_4 (0.33), KH_2PO_4 (0.34), glucose (10) and 2-[4-(2-hydroxyethyl)-1-piperazinyl]ethanesulphonic acid (HEPES) (11), adjusted to pH 7.4 with NaOH. Enzyme solutions were made up with 100 μM Ca^{2+} PSS. The bathing (external) solution contained (mM): NaCl (126), KCl (5), $MgCl_2$ (1), $CaCl_2$ (0.1), glucose (11), HEPES (10), adjusted to pH 7.2 with NaOH. The pipette (internal) solution contained (mM): KCl (130), $MgCl_2$ (1), ATP (Na^+ salt, 3), GTP (0.1), HEPES (10), EGTA (5) adjusted to pH 7.2 with KOH. Flecainide (Sigma, Poole, Dorset, UK) and phrixotoxin (Alomone Labs Israel through Caltag-Medsystems, UK) were dissolved in distilled H_2O as stocks of 50 mM and 1 μM, respectively, and stored at -20°C until used. Working concentrations were made up immediately before experimentation.

Statistics. Data are expressed as mean values $\pm$ standard error of the mean for the number of cells (n) analysed. Statistical significance was calculated using Student's t-test and the differences were considered significant when $P<0.05$.

Results

Depolarization of mPV myocytes from a V_H of -60 mV generated an outward current that was dominated by a slowly activating component that has been described previously (Yeung and Greenwood, 2005). However, in a number of cells a rapidly activating current was superimposed upon the delayed rectifier. This current was very prominent when a prepulse to -90 mV for 1 s was applied (see Figure 1). Digital subtraction of the currents evoked from a V_H of –60 mV from those elicited at the same V_T from –90 mV revealed a transient outward current (Figure 1c) that had a mean peak amplitude at $+20$ mV of 559 ± 37 pA ($n=48$). This transient current activated very rapidly with a mean time to peak of 4.1 ± 0.2 ms at $+20$ mV ($n=31$) and consequently for the purpose of this paper we have called the transient current, I_{UF} (ultra fast). I_{UF} also inactivated rapidly and the current decay was well fitted by the sum of two exponentials described by the time constants τ_{fast} and τ_{slow} with mean values at $+20$ mV of 8.8 ± 1.6 and 78 ± 20 ms, which represented 70.7 ± 2.7 and 29.3 ± 2.7% of the current, respectively ($n=12$). Figure 2 shows the time to peak was voltage-sensitive changing e-fold every 23 mV. The rate of

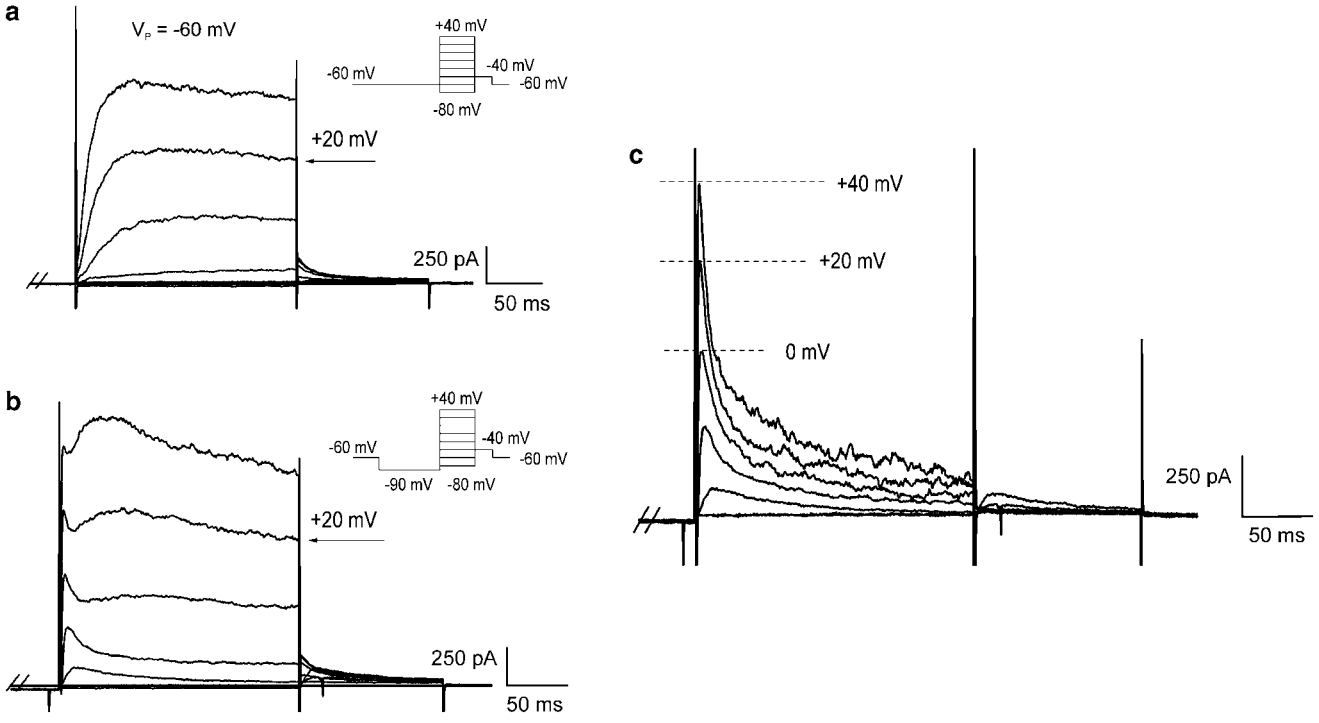

Figure 1 Isolation of I_{UF} in mPV smooth muscle cells by digital subtraction. (**a**) An example of currents evoked from a V_H of -60 mV at V_T between -80 and $+40$ mV (see insert). (**b**) Currents evoked in the same cell using a similar protocol but with a 1 s prepulse to -90 mV before the test step. (**c**) I_{UF} isolated by subtracting currents at the same V_T recorded using the protocol shown in (**a**) from those evoked using protocol (**b**).

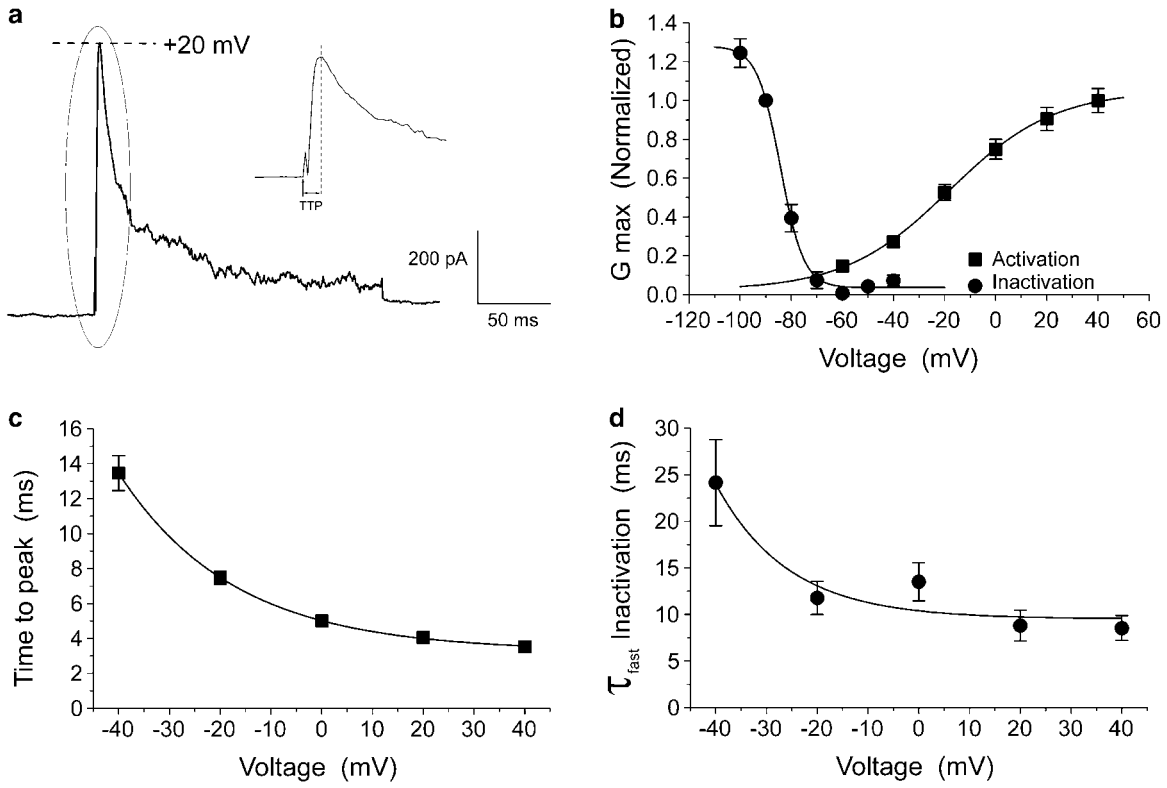

Figure 2 Voltage-dependent characteristics of I_{UF}. (**a**) An example of I_{UF} at +20 mV that illustrates the rapid rise and decay of the subtracted current. The insert shows how the time to peak (TTP) was measured. (**b**) Shows the conductance–voltage relationship for I_{UF} activation and inactivation. (**c** and **d**) Show the effect of V_T on the time to peak (**c**) and fast component of current inactivation (**d**). In each case the horizontal axis is the V_T and the vertical axis is the parameter under study.

inactivation was also voltage-dependent becoming faster with depolarization, this was due predominantly to a reduction in τ_{fast} (see Figure 2d). Experiments undertaken using a V_H of –90 mV revealed that the activation threshold of I_{UF} was about –40 mV and half maximal activation was observed at -15 ± 2.1 mV with a slope of 13 ± 2.0 mV ($n = 45$). The voltage-dependence of inactivation was determined using a two-pulse protocol and after fitting with the Boltzmann function this yielded a potential for half maximal inactivation of -83 ± 3.8 mV with a slope of 4.2 ± 0.2 mV ($n = 11$). This quantitative assessment of the availability of I_{UF} supported the initial observations that the current became manifest upon the application of a 1 s prepulse to −90 mV, highlighted in Figure 1. These experiments show that similar to rabbit portal vein myocytes a transient, voltage-dependent K^+ current was present in mPV myocytes.

Pharmacology of I_{UF} *in mPV myocytes*

As an initial step towards identifying the molecular identity of the channel underlying I_{UF} the effects of various blockers were ascertained. The channels underlying A-type currents are generally encoded by $K_v1.4$ and members of the K_v3 and K_v4 family which have a differential sensitivity to 4-aminopyridine (4-AP) with $K_v3.x$ proteins being especially sensitive (concentration that produces 50% inhibition (IC_{50}) about 0.2 μM, Coetzee *et al*., 1999). Figure 3a shows that the I_{UF} in portal vein myocytes was not particularly sensitive to 4-AP with 5 mM producing 30 ± 6% inhibition at +20 mV ($n = 11$). Flecainide is an antiarrhythmic agent that blocks sodium channels but also affects voltage-dependent K^+ channels especially those of the $K_v4.x$ family (e.g. Yeola and Snyders, 1997). Figure 3b shows that I_{UF} was very sensitive to the application of flecainide with a calculated IC_{50} of 100 nM. These data suggest strongly that the channel underlying I_{UF} is comprised of $K_v4.x$ proteins. This was corroborated with experiments with phrixotoxin II (PaTx2), a venom extracted from the spider *Phrixotrichus auratus*, which is a highly selective blocker of $K_v4.2$ and $K_v4.3$ ion channels (IC_{50} about 70 nM, Diochot *et al*., 1999). In portal vein myocytes 30 nM PaTx2 inhibited I_{UF} (Figure 3c) by 42 ± 7% ($n = 5$) at +20 mV with no apparent voltage-dependence of this effect (Figure 3ciii). These pharmacological studies suggest that the ion channel underlying I_{UF} is likely to be comprised of $K_v4.2$ or $K_v4.3$.

Expression of voltage-gated K^+ *channel genes in mPV*

Our previous studies have shown that mPV express KCNQ1 and ERG1 at relative high abundance (Ohya *et al*., 2002, 2003). We therefore undertook experiments to determine the relative abundance of the expression products for genes that encode voltage-gated K^+ channels. Figure 4a shows the results from quantitative, real-time PCR (Q-PCR) experiments undertaken on cDNA prepared from murine brain

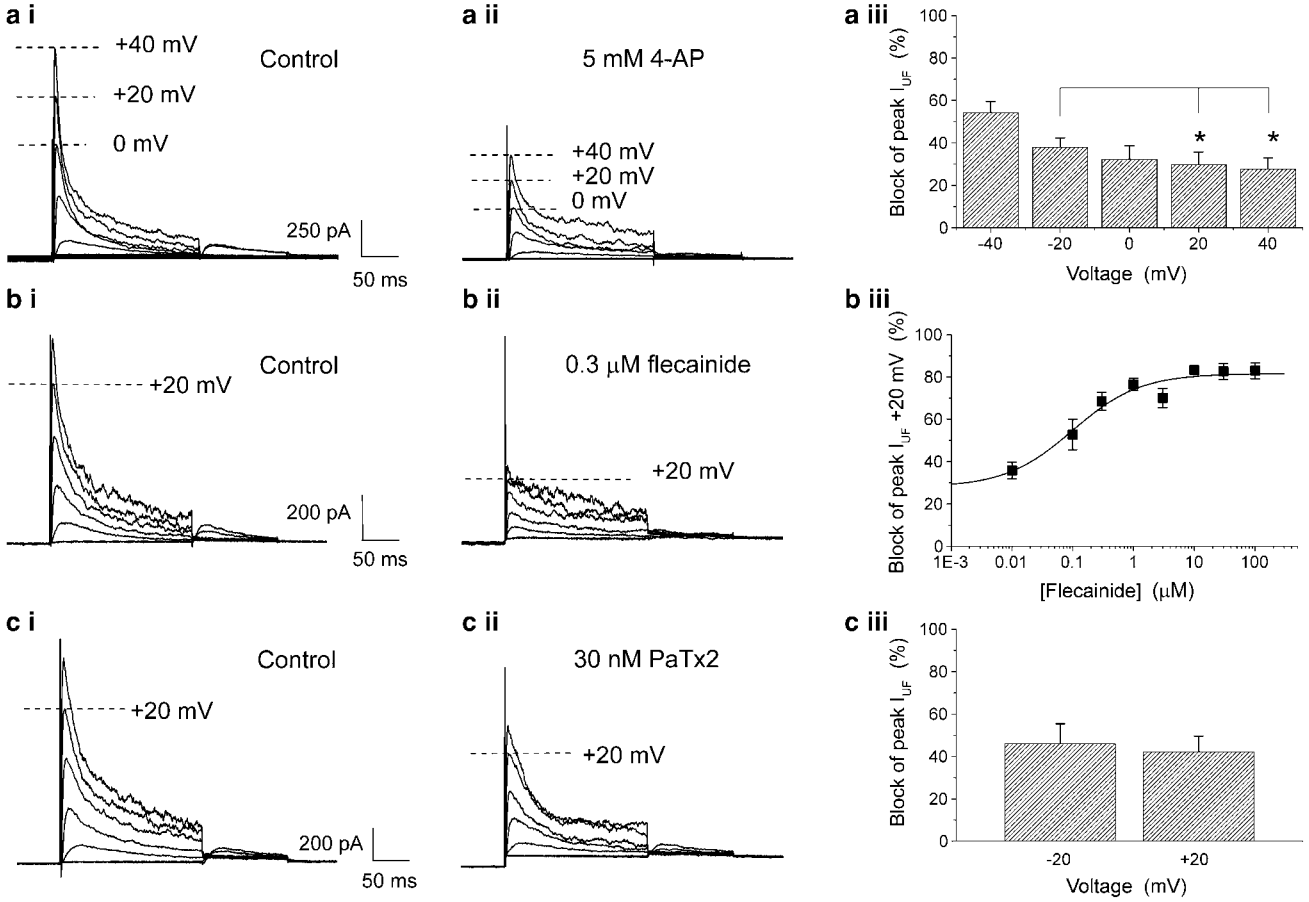

Figure 3 Pharmacology of I_{UF}. (**a–c**) Show I_{UF} evoked in three different cells at potentials between −40 and +40 mV in the absence and presence of the K^+ channel blockers (**a**) 4-AP (5 mM), (**b**) flecainide (0.3 μM) and (**c**) PaTx2 (30 nM). In each case the control currents are shown in panel (i). Panel (iii) shows mean data for the effect of (**a**) 5 mM 4-AP, (**b**) flecainide and (**c**) 30 nM PaTx2. Each value is the mean of at least five cells±s.e.m.. In panel **a** (iii) * shows significant difference ($P<0.05$) in inhibition between −20 and +20 mV and −20 and +40 mV.

that shows that expression products were obtained for all the primer sets that were used except for $K_v1.7$. In contrast Q-PCR of mPV cDNA revealed that the most abundant α-subunits were $K_v1.7$ and $K_v4.3$ (Figure 4b). The relative transcriptional expression to GAPDH was 0.013±0.0003 and 0.007±0.0002 for $K_v1.7$ and $K_v4.3$, respectively ($n=4$ for each). A $K_v\beta$-subunit, $K_v\beta3$ was also abundantly expressed in mPV, and the expression was 0.063±0.002. The expression of other K_v channel subtypes examined was less than 0.002. As smooth muscle expresses a longer splice variant of $K_v4.3$ ($K_v4.3L$, Ohya *et al*., 1997 GenBank accession number NM_019931) we used PCR primers for the splicing region of murine $K_v4.3$ that generated different size products (256 bp for $K_v4.3$ and 313 bp for $K_v4.3L$), which showed that only the longer product was apparent after 35 cycle PCR (data not shown). We also confirmed that there was no contamination with genomic DNA in mPV cDNAs by this PCR cloning (not shown). These molecular studies corroborated the pharmacological implication that $K_v4.3$ generated I_{UF}.

To ensure that $K_v4.3$ was expressed in the PV myocytes we undertook immunocytochemical experiments using an antibody raised against $K_v4.3$. Figure 5 shows that mPV smooth muscle cells stained positive for $K_v4.3$ ($n=12$ cells). The fluorescent signal was located predominantly within 1.1 μm of the plasma membrane, with significantly less signal originating in the cytoplasm deeper than this value (98.2±0.5 %FP in the Region 1 vs 51.4±5.4 %FP in the Region 2, $P<5\times10^{-6}$, or vs 55.6±4.2 %FP in the whole confocal plane of the cell, $P<5\times10^{-7}$, Student's paired *t*-test, $n=12$ cells, Figure 5a and d, also Figure 5b). The specificity of antibodies was confirmed by incubation with the antigenic peptide (1:2 ratio of antibody to antigenic peptide), which resulted in almost complete suppression of fluorescence (1:100 dilution: from 61.1±5.5 IU/pixel, $n=6$ to 3.3±0.5 IU/pixel, $n=6$, $P<5\times10^{-6}$; 1:200 dilution: from 38.4±9.6 IU/pixel, $n=6$ to 3.2±0.2 IU/pixel, $n=6$, $P<0.005$, Student's unpaired *t*-test, Figure 5c and e). The control incubations with either primary or secondary antibodies alone (Figure 5e, rightmost columns in the graph) resulted in virtually no fluorescence (APF<2.0 IU/pixel in both cases; primary antibodies $n=6$, secondary antibodies $n=6$). Consequently, murine PV myocytes express $K_v4.3$ at a high level and the protein is localized predominantly in the plasmalemma.

As various members of the recoverin–neuronal calcium binding protein superfamily (NCBPs) especially NCS1 and various KChIPs (K^+ channel interacting protein) alter the

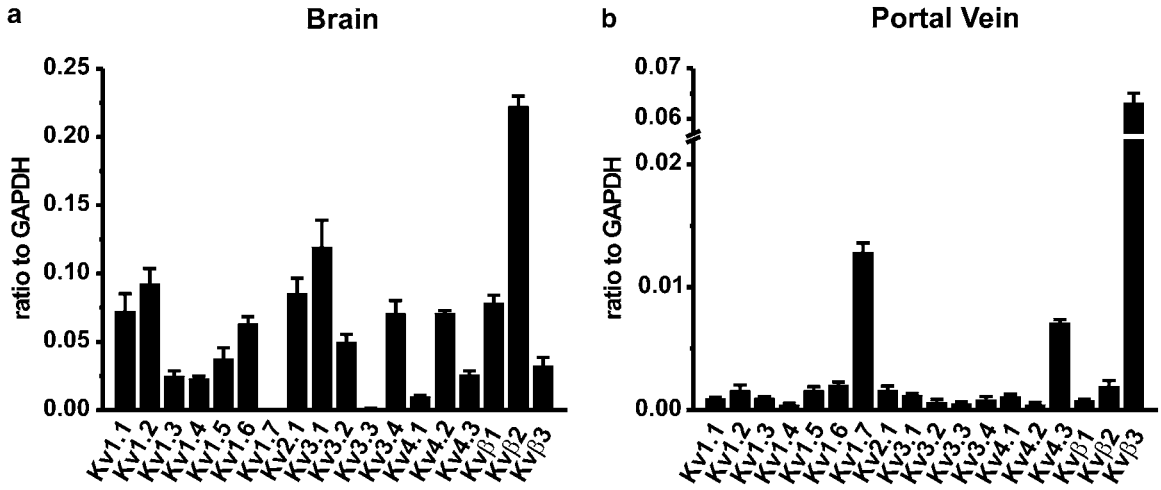

Figure 4 Quantitative, real-time PCR for Kv channel expression relative to GAPDH in mPV. (**a** and **b**) Show the summarized data for Q-PCR in murine brain (positive control) and portal vein, respectively. Values are shown for steady-state transcripts relative to GAPDH in the same preparation. Results are expressed as means ± s.e.m.

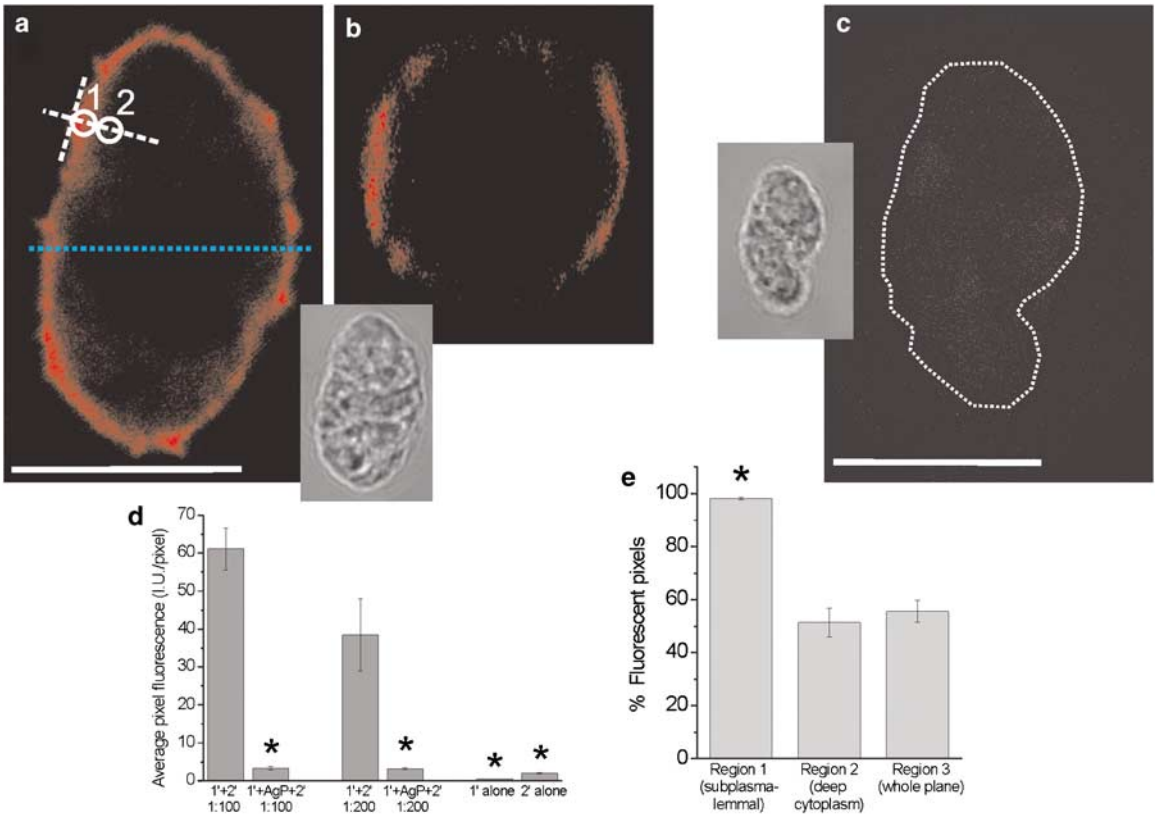

Figure 5 Immunocytochemical staining of mPV smooth muscle cells for K_V4.3 subunit of voltage-dependent potassium channel. Fluorescence images of a single confocal plane of the cell labelled with (**a**) K_v4.3 antibodies; (**b**) a vertical section through the same cell showing localization of fluorescence at the edge of the cell thought to be the plasma membrane; (**c**) K_v4.3 antibodies preincubated with their antigenic peptide. White circles in (**a**) indicate Regions 1 and 2, which were used to analyse the localization of fluorescence (for details see Methods). A dotted line was used in (**c**) to outline the contour of a cell, due to its low fluorescence. Insets in (**a**) and (**c**): transmitted light images of respective cells. Calibration in (**a**) and (**c**): 10 μm. (**d**) Summary data on intensity of fluorescence, expressed as APF (intensity units per pixel). The values of all pixels in the cell's confocal plane were added up and then divided by the number of such pixels. The specificity of labelling was confirmed by virtual lack of fluorescence after pre-incubation with the antigenic peptide or in the absence of primary antibodies. (**e**) Summarized data on localization of K_v4.3 fluorescence in the cells. There was significantly more fluorescence in the Region within ~1.1 μm of plasma membrane (Region 1) than in the deep cytoplasm (Region 2) or when compared with whole confocal plane average (Region 3). *Statistically significant.

expression and biophysical properties of $K_v4.x$ channels (Birnbaum *et al*., 2004) we undertook Q-PCR experiments to investigate the expression of these genes in the murine PV. Using primers for 12 NCBP members used in an earlier study (Ohya and Horowitz, 2002), NCS1, NVP3, KChIP1 and KChIP3 signals were easily detected in whole mPV (Figure 6a), whereas weak or no signals for the other members were detected (not shown). To avoid the contamination from nonmyocytes, cell-based RT–PCR analyses were performed on freshly isolated mPV myocytes (mPVM). These studies showed that NCS1, NVP3, KChIP1 and KChIP3 signals were detected in mPVM (Figure 6b). We further examined the expression of NCBPs by Q-PCR. The relative transcriptional expression to GAPDH was 0.070 ± 0.008, 0.093 ± 0.005, 0.097 ± 0.011 and 0.051 ± 0.007 for NCS1, NVP3, KChIP1 and KChIP3, respectively ($n=4$ for each) (Figure 6c). Primers for NCBPs have been tested on murine brain and heart (Ohya and Horowitz, 2002). These data show that PV myocytes express genes the proteins of which form partners with $K_v4.3$ that may underlie native I_{UF}.

Pharmacological properties of heterologously expressed $K_v4.3$

The pharmacological and molecular data presented so far implicate $K_v4.3$ as the protein underlying I_{UF}. In a final series of experiments we investigated the sensitivity of heterologously expressed $K_v4.3$ channels to flecainide and 4-AP. Similar to I_{UF} in murine myocytes $K_v4.3$ currents activated relatively rapidly (mean time to peak at $+20$ mV was 4 ± 0.25 ms, $n=13$) and decayed in a biexponential manner with mean τ_{fast} and τ_{slow} at $+20$ mV of 23 ± 1 ms and 108 ± 8 ms ($n=9$), which represented 79.8 ± 1.2 and 20.2 ± 1.3% of the total current, respectively ($n=13$). Currents generated by the expression of $K_v4.3$ were relatively resistant to 10 mM 4-AP (Figure 7a) with currents at $+20$ mV being reduced from 4.7 ± 1.2 to 2.5 ± 0.58 nA ($n=5$). Moreover, currents generated by the overexpression of $K_v4.3$ were not particularly sensitive to flecainide (Figure 7b) with 20 μM inhibiting the current at $+20$ mV from 8.1 ± 0.45 to 2.95 ± 0.6 nA ($n=5$). These data highlight a marked discrepancy in the pharmacology of $K_v4.3$ and I_{UF} that indicate the native current is generated by a multimeric protein complex.

Discussion

Transient K^+ currents have been observed in various vascular smooth muscle cell types (see Amberg *et al*., 2003 for summary). However, there has been no attempt to

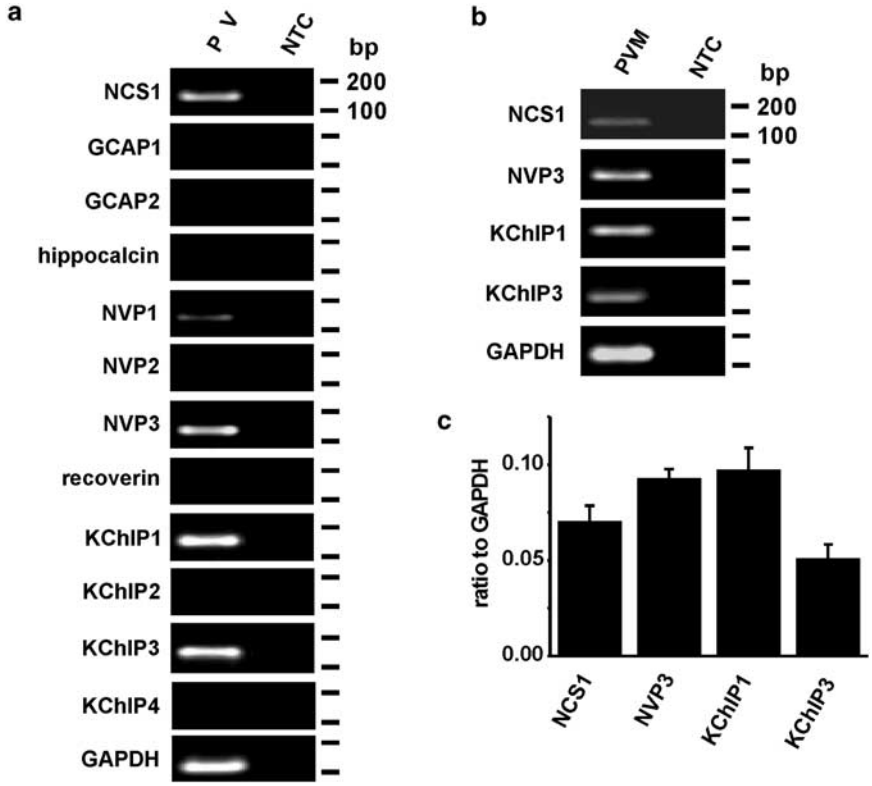

Figure 6 Transcriptional expression of neuronal calcium binding proteins in the mPV. (**a**) RT-PCR analysis of 12 NCBP members in mPV tissue (30 cycles). PCR products were generated through the use of gene-specific primers for NCS1, GCAP1-2, hippocalcin, NVP1-3, recoverin and KChIP1-4. (**b**) Cell-based RT-PCR analysis of NCBP members in mPV myocytes. PCR products were generated through the use of gene-specific primers for NCS1, NVP3, KChIP1 and KChIP3 for 40 cycles. Amplified products were separated on 2.0% agarose gels and were identified by ethidium bromide staining. 'NTC' showed the nontemplate control. A 100-bp molecular weight marker was used to estimate the size of the amplicon and the migration is shown on the right. (**c**) Summarized Q-PCR data for the expression of NCS1, NVP3, KChIP1 and KChIP3 relative to GAPDH in mPV. Values are shown for steady-state transcripts relative to GAPDH in the same preparation. Results are expressed as means$\pm$s.e.m.

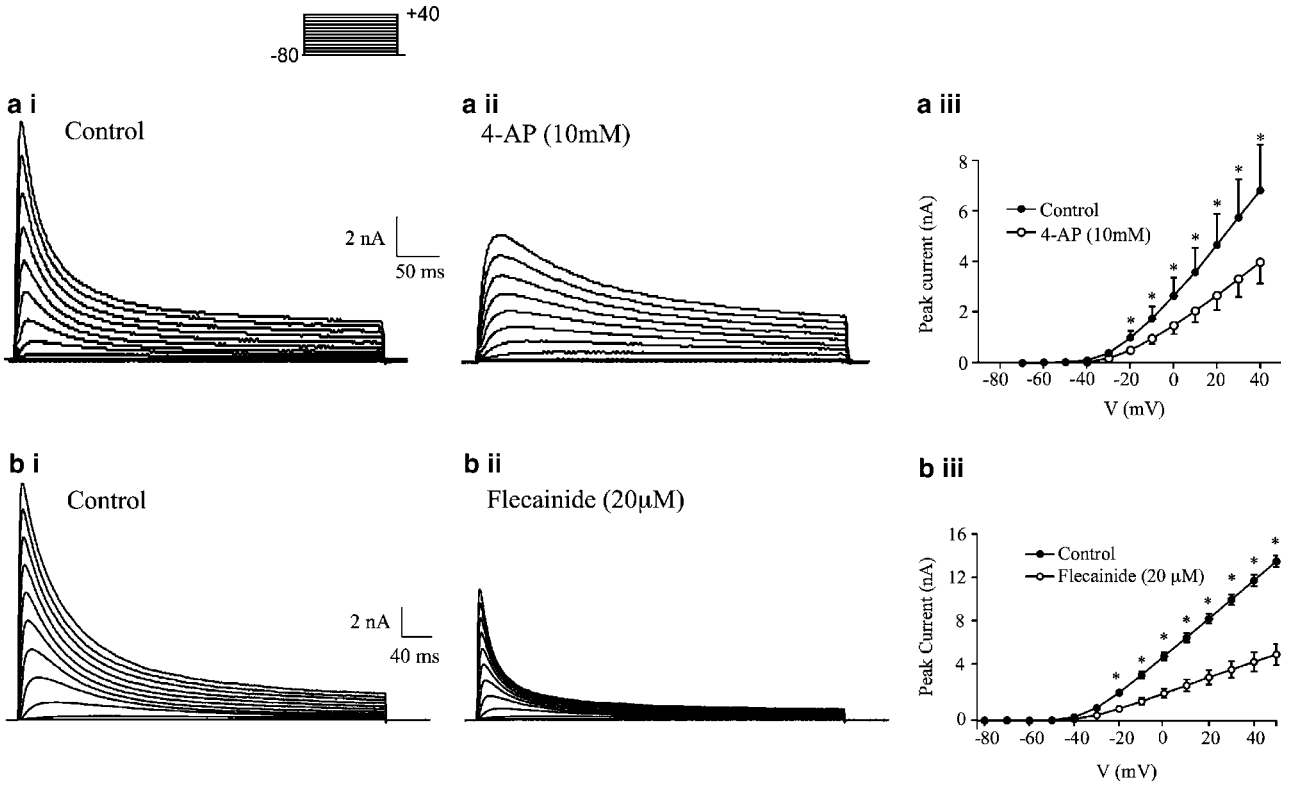

Figure 7 Pharmacological sensitivity of K_v4.3 to 4-AP and flecainide. Figures **a** (i) and **b** (i) show families of currents recorded from HEK 293 cells stably expressing K_v4.3 evoked at different potentials between −80 and + 40 mV in the absence (**a** (i), **b** (i)) and presence of 10 mM 4-AP (**a** (ii)) and 20 μM flecainide (**b** (ii)), respectively. Panels **a** (iii) and **b** (iii) show the mean current voltage relationships from five cells before (filled circles) and during addition (open circles) of 4-AP and flecainide, respectively. Error bars represent the s.e.m.

identify the molecular basis of these currents in freshly dispersed myocytes. An extensive molecular and pharmacological analysis of transient K^+ currents has been undertaken in human pulmonary artery myocytes in culture (Iida *et al.*, 2005) but there is considerable evidence that culture conditions affect the expression of pore forming proteins (Miguel-Velado *et al.*, 2005) as well as auxiliary proteins that are known to influence the surface presentation and biophysical characteristics of K^+ channels (Birnbaum *et al.*, 2004). The present study therefore represents the first attempt to identify, through pharmacological means allied to PCR and immunocytochemical methods, the protein underlying transient K^+ currents in a freshly dispersed vascular smooth muscle cells. The conclusion of these studies is that, similar to murine gastric antrum and colon (Amberg *et al.*, 2002a, b), the transient K^+ current in mPVM is likely to be generated by a channel formed from K_v4.3 proteins.

K^+ channel α-subunit expression in mPVM

Overexpression studies have revealed that transient K^+ currents can be generated by a few different α-subunits namely K_v1.4, K_v3.3, K_v3.4, K_v4.1, K_v4.2 and K_v4.3 (Gutman *et al.*, 2005). In addition K_v1.7 when coexpressed with $K_v\beta$3-subunits also produce transient K^+ currents (Coetzee *et al.*, 1999). Of these candidate genes the most abundantly expressed in the mPV were K_v1.7 and K_v4.3 with $K_v\beta$3 RNA also at high levels. As ion channels composed of K_v4.3 are relatively insensitive to 4-AP (IC_{50} ~5 mM) compared to those generated by K_v1.7/$K_v\beta$3 (IC_{50} ~0.25 mM) we used this classical K^+ channel blocker to repudiate one of the candidates. As the transient K^+ channel in the mPV was only inhibited by ~50% by 5 mM then the underlying channel is likely to be composed predominantly of K_v4.3. This was substantiated by the use of two other pharmacological agents flecainide, a Na^+ channel blocker also shown to block K_v4.*x* channels at low micromolar concentrations (Yeola and Snyders, 1997) and PaTx2, a highly selective and potent peptide inhibitor of K_v4.2 and K_v4.3 (Diochot *et al.*, 1999). Both agents inhibited I_{UF} potently with IC_{50} values for flecainide and PaTx2 of 100 and 30 nM, respectively. These data corroborate the hypothesis that a channel composed of K_v4.3 proteins generated I_{UF}. However, the pharmacological sensitivity of I_{UF} to flecainide was considerably higher than that of the currents generated by the heterologous expression of K_v4.3 in HEK cells (reported previously by Sergeant *et al.*, 2005). Furthermore, the rate of inactivation was significantly faster for the endogenous I_{UF} than for the current generated by the expression of K_v4.3. A number of proteins shown to affect the surface presentation and biophysical properties of K_v4.3 were expressed by mPVM including NCS-1, NVP3 and KChIP1. Moreover, previous studies have shown that auxiliary subunits encoded by the

KCNE gene family are also expressed by portal vein myocytes (Ohya *et al*., 2002). It is possible that the native channel is a heteromeric assembly that confers distinct biophysical and pharmacological properties. This line of investigation was out of the scope of the present study and will be the basis of future work.

Characteristics of I_{UF}

Transient A-type K^+ currents are generally found in smooth muscle cells that exhibit phasic activity. Thus, they have been characterized in myocytes from rabbit portal vein (Beech and Bolton, 1989), guinea-pig ureter (Imaizumi *et al*., 1990), pregnant human myometrium (Knock *et al*., 1999), murine colon (Amberg *et al*., 2002a) and antrum (Amberg *et al*., 2002b). In all cases the channels have a negative voltage-dependence of inactivation with $V_{0.5}$ values between -50 and -80 mV (see Amberg *et al*., 2003). I_{UF} in mPVM exhibited a similar voltage-dependence of inactivation but an activation threshold of about – 40 mV, less negative than that found in most other studies. These biophysical parameters imply that I_{UF} has little, if any, physiological role – a postulate supported to some extent by the observation that flecainide had no effect on inherent spontaneous contractions of whole mPV (I Greenwood and S Yeung, unpublished observations). This raises the question of why such a robust conductance should be present in mPVM. It is possible that the dissociation process has affected the inherent gating of the channel protein or the underlying regulatory systems have altered the channel properties. For instance, the A-type current in murine colon and $K_v4.3$ are positively regulated by the Ca^{2+}-calmodulin-dependent kinase, CaMKII (Koh *et al*., 1999; Sergeant *et al*., 2005). As the pipette solution used in the present study precluded any rise in $[Ca^{2+}]$ it is unlikely that CaMKII had any influence on membrane currents. KChIPs have a similar effect on K_v4 channels (An *et al*., 2000). The aim of the present study was not to elucidate the physiological role of I_{UF} but to identify whether $K_v4.3$ was responsible for the current observed. The conclusion is that that the underlying channel is likely to be composed of $K_v4.3$ and it remains the aim of future studies to ascertain whether A-type currents in other vascular cells have a similar molecular composition.

Acknowledgements

This work was supported by a British Heart Foundation grant (IAG), a British Heart Foundation Intermediate Research Fellowship FS/04/052 (VP) and Grant-in-Aid for Young Scientists from Japan Society for the Promotion of Science (JSPS) (14771290, SO), Gerard P Sergeant is in receipt of a Research Fellowship awarded by the Health Research Board, Ireland. We wish to acknowledge assistance by Kenton M Sanders of the University of Nevada, Reno.

Conflict of interest

The authors state no conflict of interest.

References

Akbarali HI, Thatte H, He XD, Giles WR, Goyal RK (1999). Role of HERG-like K^+ currents in opossum esophageal circular smooth muscle. *Am J Physiol* **277**: C1284–C1290.

Amberg GC, Baker SA, Koh SD, Hatton WJ, Murray KJ, Horowitz B *et al*. (2002a). Characterization of the A-type potassium current in murine gastric antrum. *J Physiol* **544**: 417–428.

Amberg GC, Koh SD, Hatton WJ, Murray KJ, Monaghan K, Horowitz B *et al*. (2002b). Contribution of K_v4 channels toward the A-type potassium current in murine colonic myocytes. *J Physiol* **544**: 403–415.

Amberg GC, Koh SD, Imaizumi Y, Ohya S, Sanders KM (2003). A-type potassium currents in smooth muscle. *Am J Physiol Cell Physiol* **284**: C583–C595.

An WF, Bowlby MR, Betty M, Cao J, Ling HP, Mendoza G *et al*. (2000). Modulation of A-type potassium channels by a family of calcium sensors. *Nature* **403**: 553–556.

Beech DJ, Bolton TB (1989). A voltage-dependent outward current with fast kinetics in single smooth muscle cells isolated from rabbit portal vein. *J Physiol* **412**: 397–414.

Birnbaum SG, Varga AW, Yuan LL, Anderson AE, Sweatt JD, Schrader LA (2004). Structure and function of K_v4-family transient potassium channels. *Physiol Rev* **84**: 803–833.

Britton FC, Ohya S, Horowitz B, Greenwood IA (2002). Comparison of the properties of CLCA1 generated currents and I_{ClCa} in murine portal vein smooth muscle cells. *J Physiol* **539**: 107–117.

Coetzee WA, Amarillo Y, Chiu J, Chow A, Lau D, McCormack T *et al*. (1999). Molecular diversity of K^+ channels. *Ann N Y Acad Sci* **868**: 233–285.

Connor JA, Stevens CF (1971). Voltage clamp studies of a transient outward membrane current in gastropod neural somata. *J Physiol* **213**: 21–30.

Diochot S, Drici MD, Moinier D, Fink M, Lazdunski M (1999). Effects of phrixotoxins on the K_v4 family of potassium channels and implications for the role of I_{to1} in cardiac electrogenesis. *Br J Pharmacol* **126**: 251–263.

Doronin SV, Potapova IA, Lu ZJ, Cohen IS (2004). Angiotensin receptor type 1 forms a complex with the transient outward potassium channel $K_v4.3$ and regulates its gating properties and intracellular localization. *J Biol Chem* **279**: 48231–48237.

Gutman GA, Chandy KG, Grissmer S, Lazdunski M, McKinnon D, Pardo LA *et al*. (2005). International Union of Pharmacology. LIII. Nomenclature and molecular relationships of voltage-gated potassium channels. *Pharmacol Rev* **57**: 473–508.

Iida H, Jo T, Iwasawa K, Morita T, Hikiji H, Takato T *et al*. (2005). Molecular and pharmacological characteristics of transient voltage-dependent K^+ currents in cultured human pulmonary arterial smooth muscle cells. *Br J Pharmacol* **146**: 49–59.

Imaizumi Y, Muraki K, Watanabe M (1990). Characteristics of transient outward currents in single smooth muscle cells from the ureter of the guinea-pig. *J Physiol* **427**: 301–324.

Knock GA, Smirnov SV, Aaronson PI (1999). Voltage-gated K^+ currents in freshly isolated myocytes of the pregnant human myometrium. *J Physiol (London)* **518**: 769–781.

Koh SD, Perrino BA, Hatton WJ, Kenyon JL, Sanders KM (1999). Novel regulation of the A-type K^+ current in murine proximal colon by calcium-calmodulin-dependent protein kinase II. *J Physiol* **517**: 75–84.

Miguel-Velado E, Moreno-Dominguez A, Colinas O, Cidad P, Heras M, Perez-Garcia MT *et al*. (2005). Contribution of K_v channels to phenotypic remodeling of human uterine artery smooth muscle cells. *Circ Res* **97**: 1280–1287.

Ohya S, Horowitz B (2002). Differential transcriptional expression of Ca^{2+} BP superfamilies in murine gastrointestinal smooth muscles. *Am J Physiol Gastrointest Liver Physiol* **283**: G1290–G1297.

Ohya S, Horowitz B, Greenwood IA (2002). Functional and molecular identification of ERG channels in murine portal vein myocytes. *Am J Physiol Cell Physiol* **283**: C866–C877.

Ohya S, Sergeant GP, Greenwood IA, Horowitz B (2003). Molecular variants of KCNQ channels expressed in murine portal vein myocytes: a role in delayed rectifier current. *Circ Res* **92**: 1016–1023.

Ohya S, Tanaka M, Oku T, Asai Y, Watanabe M, Giles WR *et al*. (1997). Molecular cloning and tissue distribution of an alternatively spliced variant of an A-type K^+ channel alpha-subunit, K_v4.3 in the rat. *FEBS Lett* **420**: 47–53.

Platoshyn O, Remillard CV, Fantozzi I, Mandegar M, Sison TT, Zhang S *et al*. (2004). Diversity of voltage-dependent K^+ channels in human pulmonary artery smooth muscle cells. *Am J Physiol Lung Cell Mol Physiol* **287**: L226–L238.

Saleh S, Yeung SY, Prestwich S, Pucovský V, Greenwood IA (2005). Electrophysiological and molecular identification of voltage-gated sodium channels in murine vascular myocytes. *J Physiol* **568**: 155–169.

Sergeant GP, Ohya S, Reihill JA, Perrino BA, Amberg GC, Imaizumi Y *et al*. (2005). Regulation of K_v4.3 currents by Ca^{2+}/calmodulin-dependent protein kinase II. *Am J Physiol Cell Physiol* **288**: C304–C313.

Yeola SW, Snyders DJ (1997). Electrophysiological and pharmacological correspondence between K_v4.2 current and rat cardiac transient outward current. *Cardiovasc Res* **33**: 540–547.

Yeung SY, Greenwood IA (2005). Electrophysiological and functional effects of the KCNQ channel blocker XE991 on murine portal vein smooth muscle cells. *Br J Pharmacol* **146**: 585–595.